Characteristics of Diffusion-Weighted and Blood Oxygen Level-Dependent Magnetic Resonance Imaging in Tubulointerstitial Nephritis: an initial experience.

Tao Su (tao.su@bjmu.edu.cn)
Peking University First hospital https://orcid.org/0000-0002-6857-8146
Xuedong Yang
China Academy of Chinese Medical Sciences Guanganmen Hospital
Rui Wang
Peking University First Hospital
Li Yang
Peking University first hospital
Xiaoying Wang
Peking University first hospital

Research article

Keywords: magnetic resonance imaging, diffusion-weighted, blood oxygenation level-dependent, tubulointerstitial nephritis, acute kidney injury, chronic kidney disease

Posted Date: November 10th, 2020

DOI: https://doi.org/10.21203/rs.3.rs-50263/v2

Abstract

Background: Diffusion weighted(DW) and blood oxygen level-dependent(BOLD) magnetic resonance imaging are classical sequences of functional MR,but the exploration in non-transplanted kidney disease is limited.Objects:To analyze the characteristics of apparent diffusion coefficient(ADC) and R_2* value using DW and BOLD imaging in tubulointerstitial nephritis(TIN).

Methods: Four acute TIN,thirteen chronic TIN patients and four controls were enrolled.A multiple gradient-echo sequence was used to acquire 12 T2*-weighted images for calculation of R_2* map.DW imaging was acquired by combining a single-shot spin-echo echo planar imaging pulse sequence and the additional motion probing gradient pulses along the x,y,z-axes with two *b* values:0 and 200, as well as 0 and 800 s/mm^2.For ATIN,DW and BOLD magnetic resonance were performed at the time of renal biopsy(T_0) and the third month(T_3).Pathological changes were assessed semi-quantitatively.Correlation analysis were conducted within functional MR,pathological and clinical indexes.

Results: In ATIN,ADCs were significantly lower(*b* was 0,200 s/mm^2,2.86±0.19vs.3.39±0.11,*b* was 0,800 s/mm^2,1.76±0.12vs.2.16±0.08,P<0.05) than controls,showing an obvious remission at T_3.Cortical and medullary R_2* values(CR_2*,MR_2*) were decreased,significantly recovery at T_3 was only observed in MR_2*(T_0 24.3±2.1vs.T_3 32.4±6.6,P<0.05).No relationship was found between fMR and histopathological indexes.MR_2* had a close relationship with eGFR(R=0.80,P=0.017) and serum creatinine(R=-0.502,P=0.012).Patients having lower ADC when *b* was 0,200 s/mm^2,showed more increase of ADC(R=-0.956,P=0.044)and MR_2*(R=-0.949,P=0.05).In CTIN group, reduced MR_2* was disclosed with unchanged CR_2* and ADC value.

Conclusions: We observed reduction and partial remission of ADC and R_2* values in ATIN.Lower ADC when *b* is 0, 200 s/mm^2 is an index indicating reversible injury.MR_2* serves as a promising marker reflecting renal function.The pseudo normalization of CR_2* with reduced MR_2* in CTIN produces an evidence of intra-renal oxygen adaptation that contributing to CKD deterioration.

Background

Functional magnetic resonance (fMR) imaging has recently grown to be a useful tool to evaluate real-time renal function[1]. The functional MR sequences mainly include blood oxygen level-dependent (BOLD), diffusion-weighted (DW) imaging, arterial labeling perfusion (ASL) and dynamic contrast-enhanced imaging (DCI). They provide information about diffusion, perfusion, and oxygenation of kidneys besides morphological parameters. These novel techniques serve as promising markers helping to further understand pathophysiology of acute kidney injury (AKI) and chronic kidney disease (CKD)[2-6]. Functional MR is also recommended for early differentiation diagnosis of renal dysfunction after kidney transplantation[7-8]. Researches with fMR were still exploratory in animal models of AKI and some human observational studies[9-11], in human studies of CKD trying to compare fMR parameters with renal pathological index[3,9]. It can be seen that the characteristics of fMR in non-transplantation human kidney diseases by contrast, were poorly understood and controversial yet.

DW and BOLD from magnetic resonance imaging are early used techniques. The apparent diffusion coefficient (ADC) calculated from DW images is influenced by both pure diffusion and perfusion-dependent diffusion at a low *b* value. It is regarded as a potential biomarker to alterations in the renal interstitium, perfusion and water handling in the tubular compartment, for example interstitial fibrosis. DW imaging is a promising tool for the diagnosis of acute renal transplant dysfunction[12]. The ADC value was observed to decrease associated with severity of renal dysfunction and degree of renal fibrosis after AKI[13]. In diabetes nephropathy, correlations were found significantly between ADC and estimated GFR values, negative with clinical stages and urinary albumin excretion[14]. A recent study reported that combination of renal ADC and parenchymal volume can improve assessment of renal function in CKD[15]. But in another CKD rat model, ADC values could not reflect degree of kidney fibrosis[10]. BOLD MR imaging was demonstrated to effectively detect changes in intra-renal oxygenation by measuring the R_2* levels of the renal cortex and medulla[9]. Li et al. observed the immediate increase in R_2* in the renal inner stripe of the outer medulla after the injection of contrast agent, which suggesting existence of tissue hypoxia probably induced by hypoperfusion[16], that BOLD served as an early biomarker of contrast induced AKI. In CKD patients with renovascular stenosis, renal oxygenation was found to decrease after furosemide injection as a result of increased oxygen consumption of tubular Na-K transporter working[17]. While in another report, renal BOLD MR imaging was found not reflecting renal function in CKD [18]. In fact, although some researchers recommend direct methods such as phase-contrast MR imaging to measure renal artery blood flow (RBF) as a surrogate for BOLD, previous analysis[17] failed to demonstrate associations between R_2* and RBF or sodium absorption. One possible explanation lies in that RBF doesn't equal to regional perfusion, and that reductions of GFR and reabsorbed sodium are more than that of RBF in CKD. A later study revealed that a better correlation existed between GFR and RBF in CKD with higher GFR, while was poor with lower GFR[19]. Gomez SI et al [20] observed increased hypoxia and reduced renal tubular response to furosemide detected by BOLD MR imaging in swine renovascular hypertension. And the difference between stenotic and contralateral kidneys was marked in animals with low Furosemide-induced suppression of oxygen consumption (22± 6 vs. 66 ± 4 ml/min, P < 0.05). Therefore, the detection of oxygenation by R_2* still has its clinical value in evaluating renal function. Furthermore, intra-renal change of oxygenation contributes to progression of CKD[21].

The pathogenesis of tubulointerstitial disease lies in damage of tubules, changes of inflammation, edema or subsequent fibrosis involving corresponding interstitial regions, and following regulation of intra-renal microcirculation, while glomeruli are initially intact[22]. Besides, tubulointerstitial changes subsequent to kinds of glomerular diseases also play a key role of disease progress. This is a perfect disease model for initial study of functional MR characteristics. The aim of this study was to observe the characteristics of BOLD and DW magnetic resonance imaging both in patients with acute and chronic tubulointerstitial nephropathy (TIN).

Methods

Patients

Patients with acute tubulointerstitial nephritis (ATIN) matched 1: 2: 1 with chronic tubulointerstitial nephritis (CTIN) and healthy control were enrolled in this study from Jan 2008 to Jan 2009. ATIN patients were included if they (a) were adults diagnosed with biopsy-proven ATIN, (b) were capable to undergo fMR examination three days within percutaneous renal biopsy, (c) had no signs of other kidney diseases both clinically and pathologically. CTIN patients were selected from our specialty clinic for all-cause tubulointerstitial nephritis (TIN) diseases. Patients were included if they (a) were adults clinically diagnosed with CTIN, (b) clinically had no signs of other kidney diseases, and been followed up for more than one year, (c) with a stable serum creatinine level at CKD stage 2-5 [23]and well-controlled hemoglobin level in the recent three months. Healthy volunteers were recruited if they (a) were adults with no history of renal or cardiac diseases, and (b) had normal serum creatinine concentrations one week before MR scanning. Patients with renal malignancy, malformation, and history of partial nephrectomy were excluded from the study. Patients with history of a diurectic use within one week before MR imaging were also excluded. For ATIN patents, serum creatinine (SCr) and hemoglobulin were routinely performed for six months (T6). BOLD and DW imaging were performed at the time of renal biopsy(T0) and the third month after supportive therapy(T3).

This prospective study was in compliance with the declaration of Helsinki, and approved by the Human Ethics Committee of Peking University First Hospital. All subjects provided written informed consent and were compatible with MR scanning.

MR imaging

All patients underwent MR imaging with a 3.0-T MR scanner (General Electric Medical Systems, Milwaukee, WI, USA). A multiple gradient-echo (mGRE) sequence was used to acquire 12 T2*-weighted images for calculation of R_2* map. The parameters of sequence were as follows:TR/TE/Flip angle/BW/matrix/ thickness/gap=100ms/6.7-32.1ms(12echoes)/45^0/31.3kHz/128×96/5mm/1mm.NEX=1, and five to 6 axial slices were acquired within one breath hold 24 seconds. DW imaging was acquired by combining a single-shot spin-echo (SE) echo planar imaging (EPI) pulse sequence and the additional motion probing gradient (MPG) pulses along the x, y, z-axes. The parameters were as follows: TR/TE/BW/matrix = 2300ms/56.1ms/250kHz/128×128. NEX=2, and the slice position was identical to the BOLD imaging by the “copy” function embedded in the MR scanner, which were scanned within 18 seconds. We used two different b value group:0 and 200s/mm^2 as well as 0 and 800 s/mm^2. Axial images were acquired for both BOLD and DW images.

Both R_2* map and apparent diffusion coefficient ADC map were generated on an AW 4.2 workstation (General Electric Medical Systems, Milwaukee, WI, USA) using “Functool” software. The reader was blinded to the subject’s clinical information. At least 8 regions of interest (ROIs), each area of which was at least 10 pixels, were carefully placed on the cortex and medulla on the corresponding anatomical template separately (using image of TE=32.1ms as a template), the measured slices covered most part of the kidney. Because of the poor resolution of the images, particularly in severe renal impairment patients, it was not possible to reliably discriminate between the cortex and the medulla, which meant that the ROIs could not be reliably placed. Hence it was only possible to calculate global ADCs for each kidney. The ROIs were manually delineated in the parenchyma of the kidneys. Both R_2* and ADC values were read out on the corresponding R_2* and ADC map [Fig 2-3]. The cortical and medullary R_2* as well as global ADC of kidney were calculated separately for each side.

Pathology

Renal tissues from four ATIN patients were handled routinely by Haemotoxylin-Eosin, Masson’s trichrome, periodic acid-Schiff, and periodic acid-silver methenamine staining for light microscopy examination. The tissue core was often obtained at depths of about 1 cm. The histopathological indexes included tubular injuries (tubular epithelial cells atrophy, vacuolar degeneration, brush border shedding, necrosis and tubulitis) and interstitial changes (edema, inflammation and fibrosis). Area and degree of tubular brush border shedding, atrophy and interstitial change were semiquantitatively assessed as scores 1, 2, 3 and 4 corresponding to not, mild, moderate and severe changes by two difference pathologists referring to a modification of the Banff Working Classification[24-25]. They were also blind to the clinical data. The activity index was the total of the scores for tubular injuries, interstitial edema, and inflammatory infiltration. The chronicity index was the total of the scores for tubular atrophy and interstitial fibrosis.

Statistical analysis

Statistical analyses were performed using the software SPSS Version 20.0 (IBM Corp., Armonk, NY). Data were presented as the median and range. Differences between groups were analyzed by the non-parametric Kruskal-Wallis test. Correlations were assessed according to the Pearson test for parametric data and the Spearman test for non-parametric data. The correlations between serum creatinine, eGFR, albuminuria and the fMR parameters (kidney volume, ADC value and R_2* value) of all kidneys were determined. The correlations between pathological indexes and fMR parameters were also analyzed. A P-value less than 0.05 was defined as statistically significant.

Results

Clinical and pathological characteristics

There were altogether 20 individuals recruited for this study, including 5 ATIN patients, 15 CTIN patients, and 5 healthy control. Four patients were excluded from the study because the quality of their fMR images was poor to be used(Fig 1. flow chart). Four patients with ATIN, thirteen patients with CTIN, and four healthy control were finally enrolled. The demographic and clinical data of the subjects are summarized in table 1. The ATIN patients were 43.8±19.4 years old, with an averaged 52.0±13.3 years old of CTIN patients. All the ATIN patients experienced acute kidney injury (AKI) defined using the Kidney Disease: Improving Global Outcomes (KDIGO)[26-27] criteria and consensus report of the Acute Disease Quality Initiative 16 Work group. There were two patients in AKI stage 1, two in AKI stage 2 and one in AKI stage 3. Renal pathology revealed that in ATIN kidneys, the glomeruli were relatively intact. Focal or diffuse tubular injuries, and diffuse interstitial edema and mononuclear cells infiltration were predominant pathological findings[Fig 4]. The activity index was averaged 12.8±3.3, with the chronicity index 3.5±0.6. Urinary albumin was increased to an average of 102.0 ± 65.9 mg/L. The Scr level was 112~401μmol/l (217.4±126.4 μmol/l, eGFR 37.4±31.5 ml/min/1.73m^2) at the time of renal biopsy, and gradually declined to normal level after short-term steroids administration during the following three months, the eGFR was averaged 65.5±29.0 ml/min, 74.4±41.1 ml/min at the third (T_3) and sixth month (T_6). The hemoglobulin of ATIN patients was 99.0±13.4 g/L initially, and corrected to 129.0±13.2 g/L.

Thirteen patients with CTIN were from our out-patient specialty for tubulointerstitial nephritis under integrative supportive therapy for CKD. The renal function was stable the recent three months before MR imaging. Patients were in CKD stage 2~5 non-dialysis, whose eGFRs were averaged 34.7±21.9 ml/min (Scr 102~526 μmol/l). Urinary albumin was 30.0 ± 17.5 mg/L. Renal anemia of CTIN patients had already been corrected to 126.8±16.8 g/L, which was matchable with healthy control.

Functional MR imaging features

In control kidneys[Fig 5], the outline was smooth and there was clear differentiation between renal cortex and medulla on T_1-weighted SE and IR sequence. The averaged volume of kidneys was (144.6±16.8)×10^3 mm^3. Global ADC values of DW imaging was 3.39±0.11 and 2.16 ±0.08 respectively when *b* value was 0, 200 or 0, 800 s/mm^2. Cortical R_2* value calculated from BOLD MR imaging was 19.7±2.1 Hz, that was obviously lower than medulla [(33.1±4.1) vs. (19.4±1.9) Hz, p<0.05] .

In ATIN patients, swollen kidneys were observed [Fig 6]. The volume was (176.8±82.8)×10^3 mm^3. ADC values obtained in DW imaging both when *b* value 0, 200 s/mm^2 and 0, 800 s/mm^2 were used, were all found to have significant decreases as 18.5%, 15.6% respectively than control group (Table 1). And obvious rising of decreased ADC values were observed following improvement of renal function to achieve a 93.5%, 100% recovery at the third month (see Table 1). Both cortical and medullary R_2* values of ATIN kidneys were also lower than controls at the time of renal biopsy, the differences was significant in MR_2* values as 26.6% (difference in CR_2* values was 10.7%). The medullary R_2* values firstly went back to a level similar as control, while the cortical R_2* values remained low (92.9% of control). For CTIN patients [Fig 7], extremely shrink kidneys with irregular outlines were found (fig 2). The volume was 89.0±23.0×10^3 mm^3. Both ADC values when *b* value 0, 200 s/mm^2 and *b* value 0,800 s/mm^2 were similar as healthy control. In R_2* map, medullary R_2* value of CTIN kidneys was averaged 28.0±5.0 Hz, which was lower than control but the difference was not statistically significant.

Further analysis disclosed that neither ADC values nor R_2* values, was correlated to histopathological indexes including tubular injuries (tubular epithelial cells atrophy, vacuolar degeneration, brush border shedding, necrosis and tubulitis) and interstitial changes (edema, inflammation and fibrosis) when compared separately. We also found no relationship within ADC values, R_2* values, AI and CI. It seems that ADC and R_2* values changed along with that of renal function (Table 1) in ATIN kidneys, while close relationship was only identified in MR_2* values with eGFR (R=0.8, P=0.017) and Scr (R=-0.502,P=0.012). The situation was similar whether for CTIN patients (R=0.615, P=0.025) or all TIN patients (R=0.682, P=0.001). ADC when *b* was 0, 800 s/mm^2 in ATIN kidneys was negatively correlated with albuminuria (R=-0.951, P=0.001), while there was no such relationship with CTIN. ATIN Patients having a lower ADC when *b* value was 0,200 s/mm^2, showed more significant changes of ADC (ΔADC, the change of ADC value over the following three months, R=-0.956, P=0.044) and MR_2* (ΔMR_2* , R=-0.949, P=0.05) after therapy. ΔADC *b* value 0,200 s/mm^2, was also correlated to the change of medullary R_2* values (ΔMR_2*, the change of MR_2* value over the following three months, R=0.995, P=0.005), which was regarded as a marker mainly affected by blood perfusion. Renal long-term prognosis analysis among candidate

predictive markers showed that no relationship was found with time-point ADC or R_2* values, but as MR_2* having a significant correlation to eGFR and Scr levels as above mentioned, it was speculated that more lower the ADC value (*b* was 0, 200 s/mm^2) was, the greater increase of ADC and MR_2* after therapy, more decrease of Scr level would be. In ATIN kidneys, a significant reduction of medullary R_2* value and ratio of MR_2* to CR_2* were detected. The rapid and reversible change of the medullary R_2* value suggested that the tubular injury was mainly caused by ischemic factors.

Although both CR_2* and MR_2* were decreased than those of healthy control at ATIN, their changes after treatment were varied, with further decline of CR_2* in two patients; in the CTIN group, only a low level of MR_2* was observed while CR_2* could remain at the normal level. These suggest that there might be a delayed recovery of AKD injury, and the "pseudo normalization" of CR_2* is caused by oxygen adaptation changes during CKD.

Discussion

In this study, we assessed kidneys of ATIN presenting acute kidney injury and CTIN kidneys of stable renal function with DW and BOLD MR imaging. The correlation of functional MR parameters with critical pathological and clinical factors indicate the potential significance of these novel techniques as noninvasive methods, contributing to diagnosis, long-term prognosis assessment and further understanding of kidney diseases.

Diffusion-weighted MR imaging yields the ADC value as an index reflecting microenvironment of diffusing water molecules. It is considered as a simple marker reflecting tissue microstructure. In case of renal dysfunction, tubular injuries lead to reduced water reabsorption process resulting in decreased diffusion[28]. Factors involving microcapillary perfusion, status of tissue edema and fibrosis also theorically dedicate to ADC. Boor P et al [10] observed ADC values in unilateral ureteral obstruction rat model, and found that renal ADCs postmortem dropped almost 75% off than baseline in vivo, suggested the leading role of perfusion contributing to ADC value especially when *b* value <200 s/mm^3. Oppositely when *b* level was higher than 400 s/mm^3, ADC value declined only 25%, because the value was mostly generated from the effect of diffusion. Xu Y et al [29] reported that ADC values of impaired kidneys (when *b* was 500) were significantly lower in a linear but positive correlation with eGFR in patients mainly with renal arterial stenosis. In the current study, we revealed similar level of the global ADC values in CTIN patients as control. While there were obviously decreased but reversible changes of ADC values when *b* is 0, 200 and 0, 800 s/mm^2 in patients with ATIN, when compared with control. Presumably this indicated that there was redistribution of intra-renal micro-circulation in the background of interstitial inflammation leading to reduced blood perfusion, and decreased water diffusion because of tubular injuries, thus ADC in both low and higher *b* values declined. The delayed recovery of ADC (especially when *b* was 0, 200 s/mm^2) meant that kidney injury was still in the process of repair or left behind chronicity. After that, the kidney was likely to undergo adaptive changes continually, and when it finally reached a stable CKD stage, as data shown in CTIN patients, ADC could approach normal level. It is concluded from the current study that lower ADC may serve as a promising marker reflecting reversible acute injury, but not sensitive for interstitial fibrosis.

As we have known, the R_2* value of BOLD MR imaging has been regarded as a factor reflecting tissue oxygenation[30]. The renal medulla is vulnerable to hypoxia because of low oxygen delivery due to low vascular density in medulla, arterial-venous shunting, and high oxygen consumption for active transcellular transport of sodium and chloride in loop of Henle. Therefore, it is not difficult to understand that oxygen consumption and R_2* values decrease due to renal tubulointerstitial injury. If the injury is mainly related to direct toxicity, it only shows the decrease of cortical R_2*[31]. However, if the mechanism of renal tubular injury is also involved in ischemic factors, such as renal ischemia with redistribution of blood flow during acute inflammation, renal artery stenosis, diabetic microangiopathy, acute rejection of graft-kidney[32] and aristolochic acid nephropathy, then the R_2* of both cortex and medulla will change. The change of medullary R_2* would happen earlier and more significant. In our study, we verified that medullary R_2* was closely correlated to eGFR for all the patients, that it can be regarded as an important marker to reflect renal dysfunction. The change of CR_2* was mild, it is because acute ischemia compromises oxygen delivery while oxygen consumption by the reabsorption is maintained. The reduction of MR_2* to CR_2* ratio was detected in ATIN, suggested that the tubular injury was mainly caused by ischemic factors. The delayed recovery of CR_2* value is due to the increase of tissue oxygenation by the improvement of blood perfusion, so the change of CR_2* was not significant. It is interesting that cortical R_2* was normalized in CTIN kidneys opposite to the persistent low medullary R_2*. And this "pseudo normalization" of CR_2* by supportive change in CTIN may be the result of the intra-renal redistribution of microperfusion, certainly will lead to aggravation of medulla ischemia and hypoxia, contributing to the deterioration of CKD.

DW MR imaging and BOLD imaging are the basic classical sequences of functional nuclear magnetic resonance in clinical application, but the exploration in the field of non-transplanted kidney disease is still limited. From the results of this study, we consider that DW combined with BOLD imaging may be helpful to judge AKD, especially the emergence of AKD on the basis of the original CKD in case of not applicable to kidney biopsy, as a non-invasive diagnostic method that can be tried. However, the response of DW MR to renal interstitial fibrosis is insensitive, because the result of patients with stage CKD3-5 showed no difference from those of normal. But the joint examination using the basic scanning sequence is one of the feasible ways that can be popularized and applied to clinic in the future.

The limitation of our study was the disability to get direct information of intra-renal perfusion, despite that DW and BOLD imaging were nowadays the most frequently used functional MR imaging techniques in human diseases. Combination of these data could indirectly to some extent reflect tissue edema, inflammation, fibrosis and even be relevant to organ dysfunction. Microcirculation might also be roughly assessed, but could not be determined histologically by routine methods. More and special multi-sequence should be researched and developed in the future in order to further understand the mechanism of diseases[33-34]. The limitation of functional MR sequence scanning also lies in the influence of respiration on the scanning image quality. For critically ill patients, the poor respiratory cooperation in the intensive care unit is a problem that restricts the clinical application of fMR.

Conclusions

In conclusion, we observed reduction and partial remission of ADC and R_2* in ATIN. Lower ADC when *b* is 0, 200 s/mm^2 is a promising index indicating reversible injury, but further sample recruitment is essential to achieve critical value and verification. The "pseudo normalization" of CR_2* with reduced MR_2* in CTIN produce an evidence of intra-renal oxygen adaptation that contributing to CKD deterioration.

Abbreviations

MR: magnetic resonance; fMR: functional MR; DW:diffuse weighted; BOLD: Blood oxygen level-dependent; ADC: global apparent diffusion coefficient; ATIN: acute tubulointerstitial nephritis; CTIN:chronic tubulointerstitial nephritis;CR_2*: cortical R_2* values; MR_2*:medullary R_2* values

Declarations

Ethics approval and consent to participate

Not Applicable.

Consent for Publication

Written informed consent was obtained from the patients for publication and any accompanying images.

Availability of data and materials

These patients were regularly followed up and the clinical data is traceable. The datasets used and analysed during the current study are available from the corresponding author on reasonable request.

Competing interests

No one of the Authors has a financial and non-financial competing interest.

Funding

This research was supported by grants from National Science and Technology Major Projects for major new drugs innovation and development (2017ZX09304028), the Beijing Young Scientist Program (BJJWZYJH01201910001006) and Peking University Clinical Scientist Program. The funders played roles in the collection of data, follow-up of the patients and interpretation of data.

Authors' Contributions

TS and LY contributed to patient diagnosis, management and clinical data analysis. XY, RW and XW contributed to analysis of functional MR imaging data and provided relating images. TS and XY wrote manuscript drafting, contributed to data analysis, interpretation and intellectual content of critical importance to the work described. LY and XW interpretation and intellectual content of critical importance to the work and revised the manuscript. All authors had the opportunity to revise the manuscript.

Acknowledgements

We gratefully thank Dr. Ju Cao and Dr. Gang Liu for her help of data collection, and Dr. Xiaomei Li for the valuable suggestion of project design. We also thank the patients for agreeing to participate in this study.

References

1. Zhang JL, Rusinek H, Chandarana H, Lee VS. Functional MRI of the kidneys. J Magn Reson Imaging. 2013,37: 282–293.

2. Prasad PV. Functional MRI of the kidney: tools for translational studies of pathophysiology of renal disease.Am J Physiol Renal Physiol. 2006,290: F958–F974
3. CaroliA,Schneider M, Friedli I, Ljimani A, De Seigneux S, Boor P, et al. Diffusion-weighted magnetic resonance imaging to assess diffuse renal pathology: a systematic review and statement paper. Nephrol Dial Transplant. 2018,33: ii29–ii40
4. Dong J, Yang L, Su T, Yang X, Chen B, Zhang J, Wang X, et al. Quantitative assessment of acute kidney injury by noninvasive arterial spin labeling perfusion MRI: a pilot study. Sci China Life Sci, 2013, 56: 745–750
5. Zhou HY, Chen TW, Zhang XM. Functional Magnetic Resonance Imaging in Acute Kidney Injury: Present Status. Biomed Res Int. 2016;2016:2027370.
6. Mao W, Zhou J, Zeng M, Ding Y, Qu L, Chen C, et al. Chronic kidney disease: Pathological and functional evaluation with intravoxel incoherent motion diffusion-weighted imaging. J Magn Reson Imaging. 2018, 47: 118-124
7. WangZJ, Kumar R, Banerjee S, Hsu CY. Blood oxygen level-dependent (BOLD) MRI of diabetic nephropathy: preliminary experience. J Magn Reson Imaging. 2011,33: 655-660
8. Palmucci S, Mauro LA, Veroux P, Failla G, Milone P, Ettorre GC, et al. Magnetic resonance with diffusion-weighted imaging in the evaluation of transplanted kidneys: preliminary findings.Transplant. Proc. 2011,43:960-966
9. Tewes S, Gueler F, Chen R, Gutberlet M, Jang MS, Meier M, et al. Functional MRI for characterization of renal perfusion impairment and edema formation due to acute kidney injury in different mouse strains.PLoS ONE. 2017,12:1-18
10. Boor P, Perkuhn M, Weibrecht M, Zok S, Martin IV, Gieseke J, et al. Diffusion-weighted MRI does not reflect kidney fibrosis in a rat model of fibrosis. J Magn Reson Imaging. 2015, 42:990-998
11. Hofmann L, Simon-Zoula S, Nowak A, Giger A, Vock P, Boesch C, et al. BOLD-MRI for the assessment of renal oxygenation in humans: Acute effect of nephrotoxic xenobiotics. Kidney Int. 2006, 70: 144-150
12. Steiger P, Barbieri S, Kruse A et al. Selection for biopsy of kidney transplant patients by diffusion-weighted MRI. Eur Radiol 2017; 27: 4336–4344
13. Hueper K, Rong S, Gutberlet M, HartungD,Mengel M, Lu X, et al. T2 relaxation time and apparent diffusion coefficient for noninvasive assessment of renal pathology after acute kidney injury in mice:comparison with histopathology. Investigative Radiology.2013,48:834842.
14. CakmakP,Yağcı AB, Dursun B, Herek D, Fenkçi SM. Renal diffusion-weighted imaging in diabetic nephropathy: correlation with clinical stages of disease. Diagn Interv Radiol. 2014,205:374-378
15. LiQ,Wang D, Zhu X, Shen K, Xu F, Chen Y, et al. Combination of renal apparent diffusion coefficient and renal parenchymal volume for better assessment of split renal function in chronic kidney disease. Eur J Radiol. 2018,108:194-200
16. LiLP, Lu J, Zhou Y, Papadopoulou MV, Franklin T, Bokhary U, et al. Evaluation of intrarenal oxygenation in iodinated contrast-induced acute kidney injury-susceptible rats by blood oxygen level-dependent magnetic resonance imaging. Investigative Radiology. 2014,49:403-410
17. KhatirDS,Pedersen M, Jespersen B, Buus NH. Evaluation of Renal Blood Flow and Oxygenation in CKD Using Magnetic Resonance Imaging.Am J Kidney Dis. 2015,663:402-411
18. Michaely HJ, Metzger L, Haneder S, Hansmann J, Schoenberg SO, Attenberger UI. Renal BOLD-MRI does not reflect renal function in chronic kidney disease. Kidney Int. 2012,81:684-689
19. AbumoawadA,Saad A, Ferguson CM, Eirin A, Woollard JR, Herrmann SM, et al. Tissue hypoxia, inflammation, and loss of glomerular filtration rate in human atherosclerotic renovascular disease. Kidney Int. 2019;954:948-957
20. GomezSI,Warner L, Haas JA, Bolterman RJ, Textor SC, Lerman LO, et al. Increased hypoxia and reduced renal tubular response to furosemide detected by BOLD magnetic resonance imaging in swine renovascular hypertension. Am J Physiol Renal Physiol. 2009, 297: F981-F986
21. Nangaku M. Chronic hypoxia and tubulointerstitial injury: a final common pathway to end-stage renal failure.J Am Soc Nephrol. 2006,17:17-25
22. SuT,Gu Y, Sun P, Tang J, Wang S, Liu G, et al. Etiology and renal outcomes of acute tubulointerstitial nephritis: a single-center prospective cohort study in China. Nephrol. Dial. Transplant. 2018,33:1180-1188
23. LeveyAS,Stevens LA, Schmid CH, Zhang YL, Castro AF, Feldman HI. A new equation to estimate glomerular filtration rate. Ann Intern Med. 2009;150:604-612.
24. SolezK, ColvinRB, Racusen LC, Haas M, Sis B, Mengel M, et al. Banff 07 classification of renal allograft pathology: updates and future directions. Am J Transplant. 2008,8:753–760.
25. RacusenLC,Solez K, Colvin RB, Bonsib SM, Castro MC, Cavallo T, et al. The Banff 97 working classification of renal allograft pathology. Kidney Int. 1999;55:713–723.

26. Kidney Disease: Improving Global Outcomes (KDIGO) Acute Kidney Injury Work Group. KDIGO practice guideline for acute kidney injury. Kidney Int suppl. 2012;2:1-138.
27. ChawlaLS,Bellomo R, Bihorac A, Goldstein SL, Siew ED, Bagshaw SM, et al. Acute kidney disease and renal recovery: consensus report of the Acute Disease Quality Initiative (ADQI) 16 Workgroup. Nat Rev Nephrol. 2017;13:241–257.
28. Morrell GR, Zhang JL, Lee VS. Magnetic Resonance Imaging of the Fibrotic Kidney. J Am Soc Nephrol. 2017,28:2564-2570
29. Xu Y, Wang X, Jiang X. Relationship Between the Renal Apparent Diffusion Coefficient and Glomerular Filtration Rate: Preliminary Experience. J Magn Reson Imaging. 2007,26:678-681.
30. Inoue T, Kozawa E, Okada H, Inukai K, Watanabe S, Kikuta T, et al. Noninvasive evaluation of kidney hypoxia and fibrosis using magnetic resonance imaging. J Am Soc Nephrol. 2011 Aug;22(8)
31. CaoJ,Yang XD, Wang XY, Qu L, Liu G, Li XM. Differential changes of intrarenal oxygenation in rat models of acute tubular necrosis caused by aristolochic acid and gentamicin. Zhonghua Yi Xue Za Zhi 2010, 90:1208-1212
32. SadowskiEA,Fain SB, Alford SK, Korosec FR, Fine J, Muehrer R, et al. Assessment of acute renal transplant rejection with blood oxygen level-dependent MR imaging: initial experience. Radiology 2005 Sep;236(3)
33. WangW,Yu Y, Wen J, Zhang M, Chen J, Cheng D,et al. Combination of Functional Magnetic Resonance Imaging and Histopathologic Analysis to Evaluate Interstitial Fibrosis in Kidney Allografts. Clin J Am Soc Nephrol, 2019,14:1372-1380
34. Liang L, Chen WB, Chan KW, Li YG, Zhang B, Liang CH, et al. Using intravoxel incoherent motion MR imaging to study the renal pathophysiological process of contrast-induced acute kidney injury in rats: comparison with conventional DWI and arterial spin labelling. Eur Radiol2016;26:1597-1605

Tables

Table 1. Laboratory and fMR data of ATIN and CTIN kidneys

	Age	Scr (μmol/l)	eGFR (ml/min)	Hb (g/L)	Cortical R_2*（Hz）	Medullary R_2*（Hz）	ADC value *b* value 800 （mm^2/s）	ADC value *b* value 200 mm^2/s）	*Volume (cm3)*
Control	50.3±10.0	60~83	90~110	135.2±5.2	19.7±2.1	33.1±4.1	2.16±0.08	3.39±0.11	144.6±16.8
ATIN T0	43.8±19.4	112~401 （217.4±126.4）	9.9~82.8 (37.4±31.5）	99.0±13.4	17.6±1.3	24.3±2.1#	1.76±0.12#	2.86±0.19#	176.8±82.8
T3		88~121 （103.3±15.8）	66.6±31.2	129.0±13.2	18.3±2.2	32.4±6.6	2.02±0.04*	3.41±0.10*	154.2±7.0
T6		76~118 （97.5±21.0）	74.4±41.1	134.8±8.6	N.D.	N.D.	N.D.	N.D.	N.D.
CTIN	52.0±13.3	102~526 （240.2±146.0）	5.1~79.8 (34.7±21.9）	126.8±16.8	19.0±2.2	28.0±5.0	2.20±0.20	3.46±0.43	89.0±23.0^
eGFR<45							2.23±0.21	3.14±0.30※	
eGFR>45							2.15±0.19	3.66±0.37	

Note: # when compared between T0 and control, the difference is significant P<0.05.

* when compared between T0 and T3, the difference is significant P<0.05.

no significant difference was found between T3 and control

※when compared with group eGFR>45 ml/min, the difference is significant P<0.05.

Figures

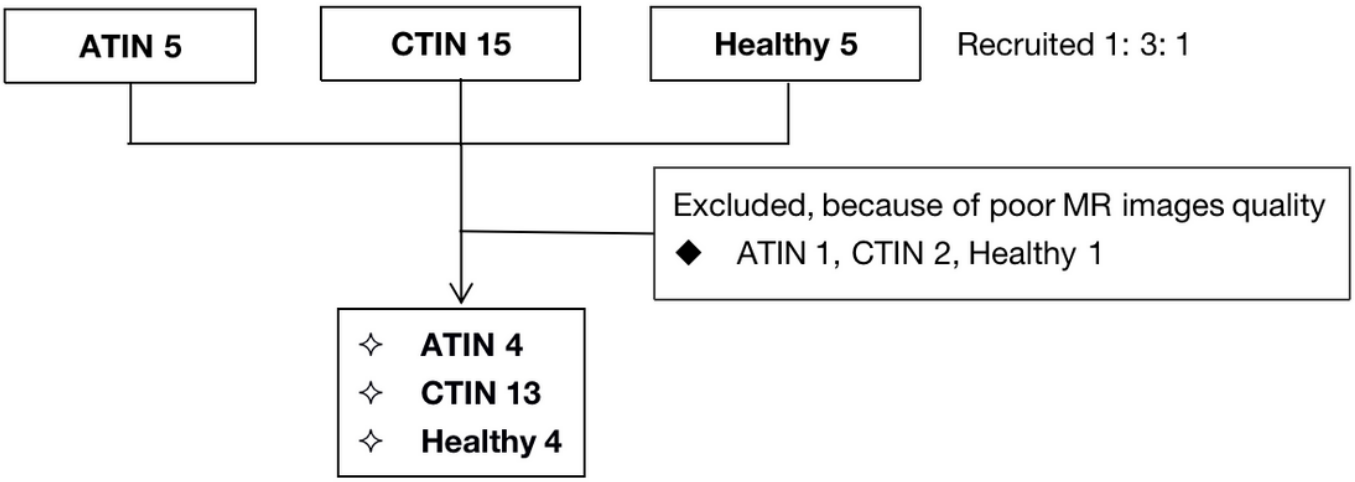

Figure 1

the flow chart of the study.

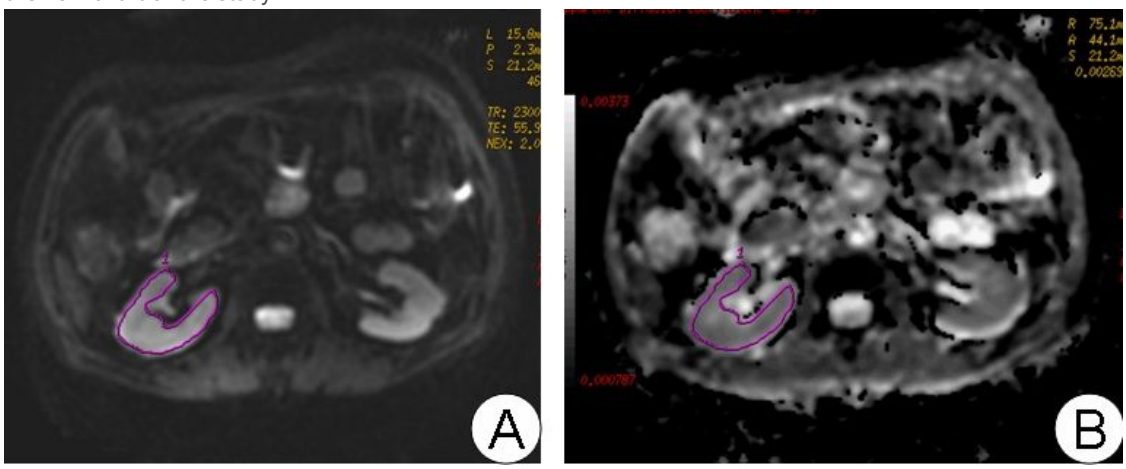

Figure 2

A:DWI image. B: the corresponding ADC diagram. The method of manual placement of ROI is used to draw the outline of the kidney on the anatomical map with (DWI).

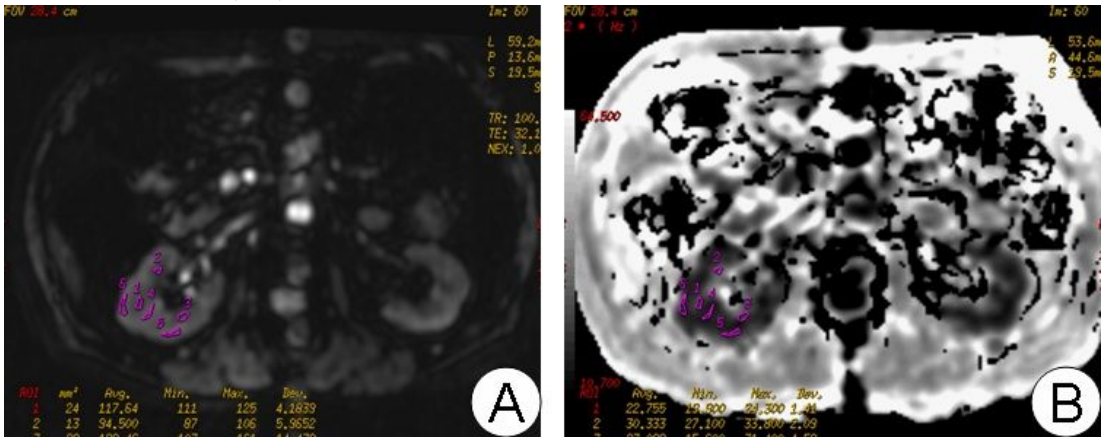

Figure 3

A:BOLD image anatomical template. BRV R2* figure. The method of manually placing ROI on the anatomical template is to place at least three ROI, in the cortical medulla and read the corresponding R2* value on the corresponding R2* diagram.

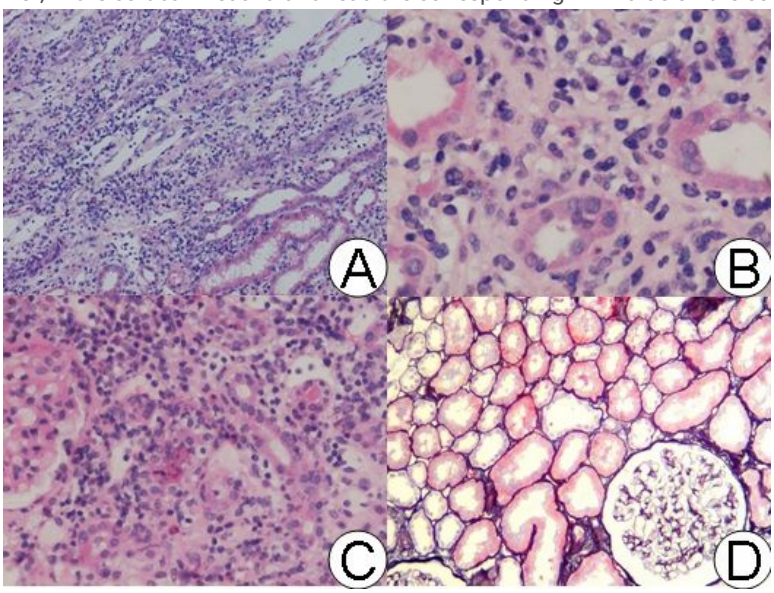

Figure 4

pathological pictures of ATIN and normal kidney (all HE staining). A: example 1, mag-nification 100xdexB: case 2, magnification x400 × C: case 3, magnification x200. From A to C, ATIN, showed exfoliated brush margin of renal tubules, dilated lumen, diffuse edema of renal interstitium, multifocal or diffuse (C) lymphoid and monocytes infiltra-tion and eosinophils infiltration. There were no obvious pathological changes in glo-meruli and arterioles. Figure D shows normal kidney, magnification x100: glomeruli and tubules are normal.

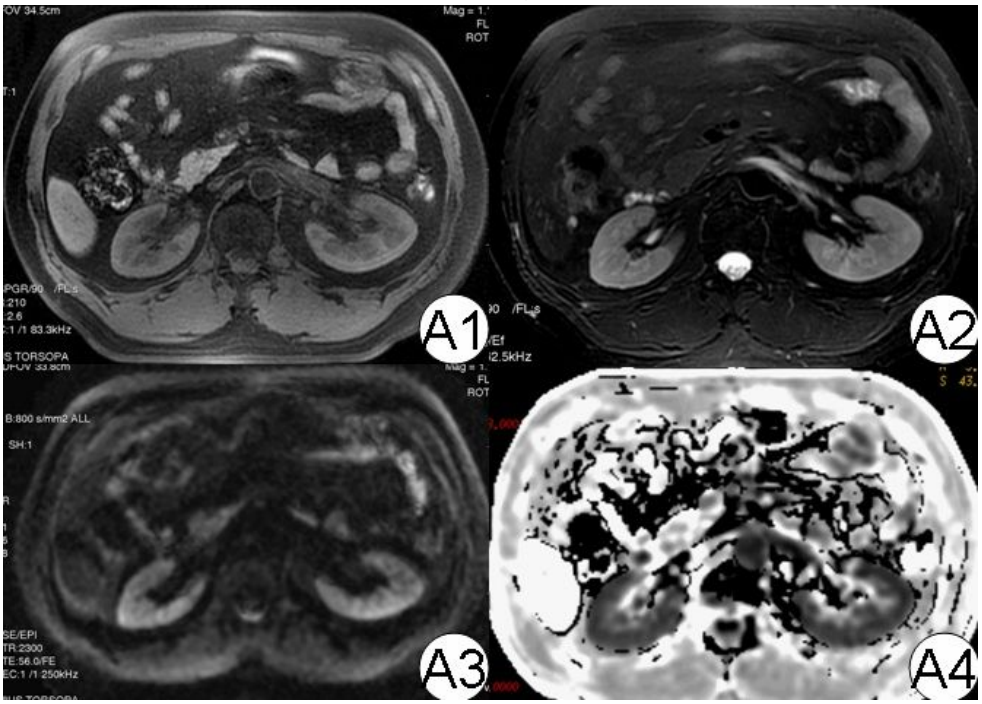

Figure 5

MRI diagram of normal kidney. In the picture, A1 to A4 are T1WI, T2WI, DWI and R2*, respectively. It can be seen that the demarcation of the epithelium and medulla on T1WI, T2WI and R2 * maps is clear (3 points).

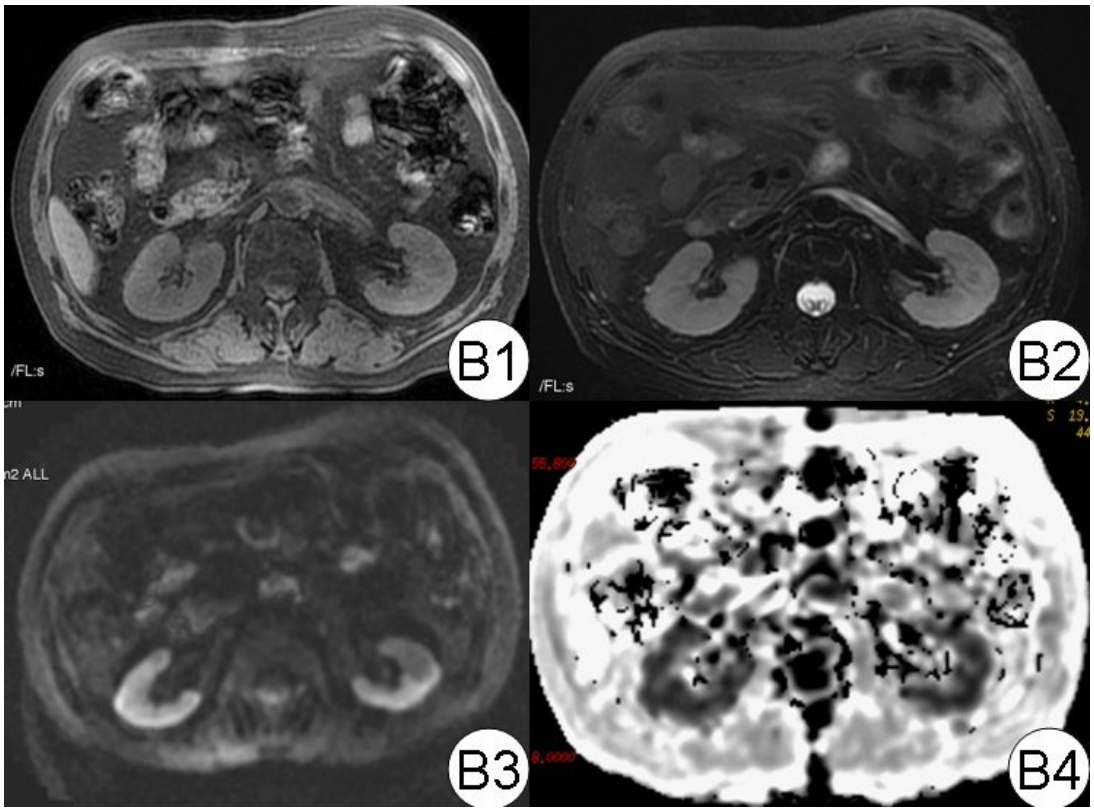

Figure 6

ATIN kidney MRI diagram. In the picture, B1 to B4 are T1WI and T2WI DWI and R2* pictures, respectively. It can be seen that the corticomedulla boundary between T1WI and T2WI is OK (2 points). Compared with normal, the cortical area of R2 * map is slightly irregular.

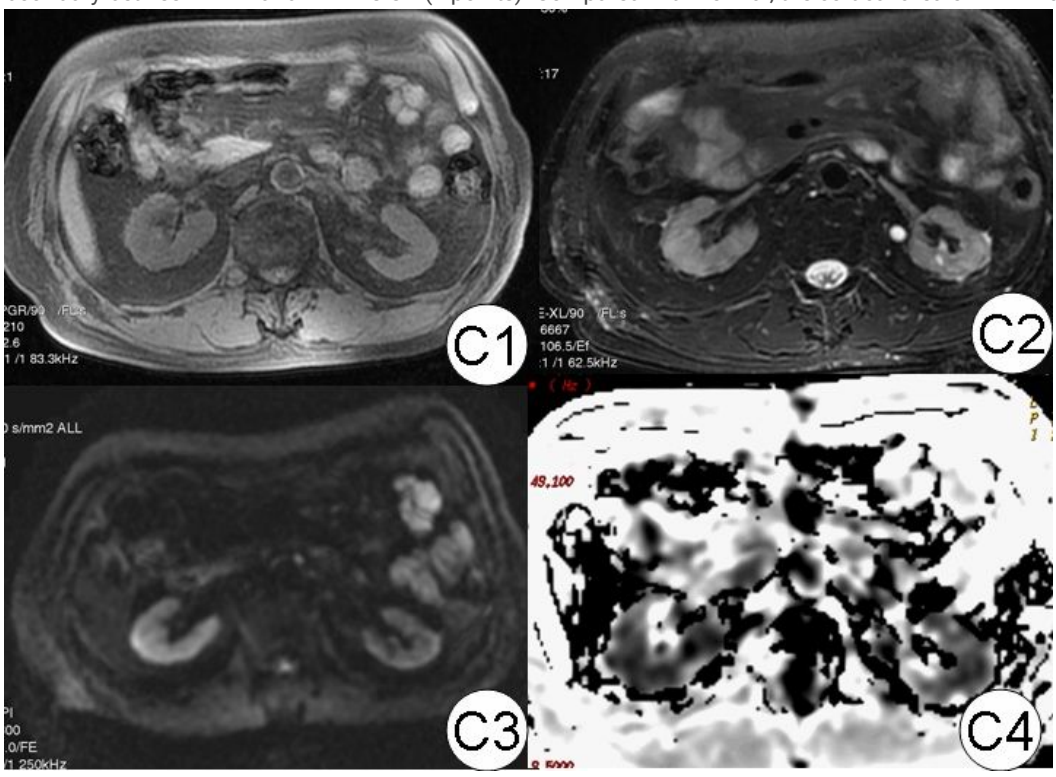

Figure 7

CTIN kidney MRI diagram. In the figure, C1 to C4 are T1WI and T2WIMagol DWI and R2* pictures, respectively. The epithelial medulla boundary of T1WI and T2WI could only be seen faintly (1 point). Compared with normal and ATIN, the epithelial medulla of R2 * was obviously irregular.